Computers & Geosciences 89 (2016) 21–31

Contents lists available at ScienceDirect

Computers & Geosciences

journal homepage: www.elsevier.com/locate/cageo

Research paper

Solid images for geostructural mapping and key block modeling of rock discontinuities

Pierre Assali [a,*], Pierre Grussenmeyer [b], Thierry Villemin [c], Nicolas Pollet [a], Flavien Viguier [a]

[a] SNCF (French National Railway Company) | Engineering Management, 6 Avenue François Mitterrand, 93574 La Plaine Saint-Denis, France
[b] ICube Laboratory UMR 7357–Photogrammetry and Geomatics Group, INSA de Strasbourg, 67084 Strasbourg, France
[c] EDYTEM | Université de Savoie Savoie Technolac, 73376 Le Bourget du Lac, France

ARTICLE INFO

Article history:
Received 20 July 2015
Received in revised form
16 December 2015
Accepted 11 January 2016
Available online 12 January 2016

Keywords:
Rock discontinuity
Structural mapping
Terrestrial laser-scanner
Solid image
Digital survey
Key block modeling

ABSTRACT

Rock mass characterization is obviously a key element in rock fall hazard analysis. Managing risk and determining the most adapted reinforcement method require a proper understanding of the considered rock mass. Description of discontinuity sets is therefore a crucial first step in the reinforcement work design process. The on-field survey is then followed by a structural modeling in order to extrapolate the data collected at the rock surface to the inner part of the massif. Traditional compass survey and manual observations can be undoubtedly surpassed by dense 3D data such as LiDAR or photogrammetric point clouds. However, although the acquisition phase is quite fast and highly automated, managing, handling and exploiting such great amount of collected data is an arduous task and especially for non specialist users. In this study, we propose a combined approached using both 3D point clouds (from LiDAR or image matching) and 2D digital images, gathered into the concept of "solid image". This product is the connection between the advantages of classical true colors 2D digital images, accessibility and interpretability, and the particular strengths of dense 3D point clouds, i.e. geometrical completeness and accuracy. The solid image can be considered as the information support for carrying-out a digital survey at the surface of the outcrop without being affected by traditional deficiencies (lack of data and sampling difficulties due to inaccessible areas, safety risk in steep sectors, etc.). Computational tools presented in this paper have been implemented into one standalone software through a graphical user interface helping operators with the completion of a digital geostructural survey and analysis. 3D coordinates extraction, 3D distances and area measurement, planar best-fit for discontinuity orientation, directional roughness profiles, block size estimation, and other tools have been experimented on a calcareous quarry in the French Alps.

1. Introduction

Rock mass engineering requires a proper understanding of site geology, rock structure, mechanical and hydrological properties. Rock outcrops consist of intact rock separated and crossed by many discontinuities. Both geometrical and mechanical characterization of intact rock properties is usually performed through laboratory tests including the quantification of compressive and tensile strengths, elastic properties, etc. Beyond these internal characteristics, describing the discontinuity structure is also a crucial input to rock fall risk analysis. According to the rock block theory (Goodman and Shi, 1985), geometrical characteristics of these discontinuities, visible at the surface of the outcrop and extrapolated to the inner part of the massif, leads to the individualization of stones, blocks and masses potentially generating disorders with variable consequences depending on their localization and their fall energy. When determining the most adapted reinforcement method (rock anchors, detection nets, etc.), fracture mapping is therefore a fundamental first step in the design process. Today, *cell mapping* or *scan line survey* (Priest and Hudson, 1981) are generally based on manual compass clinometer and tape measuring. Unfortunately, manual field survey methods have several well-known weaknesses (Kemeny and Post, 2003; Slob et al., 2005).

Digital imaging and 3D laser-scanning offer the possibility to mitigate these gaps by providing a complete and accurate 3D geometric description of the surface of the digitized outcrop. Terrestrial laser-scanning technology, also known as LiDAR (for Light Detection And Ranging) and digital photogrammetry are close-range remote sensing technologies which allow rock

* Corresponding author.
E-mail addresses: pierre.assali@gmail.com (P. Assali), pierre.grussenmeyer@insa-strasbourg.fr (P. Grussenmeyer), thierry.villemin@univ-savoie.fr (T. Villemin), nicolas.pollet@sncf.fr (N. Pollet), flavien.viguier@sncf.fr (F. Viguier).

http://dx.doi.org/10.1016/j.cageo.2016.01.002
0098-3004/

outcrops to be digitally captured in a very short time and with unprecedented resolution and accuracy (Buckley et al., 2008; Sturzenegger and Stead, 2009). Resulting 3D models can then be post-processed thanks to automated or semi-automated procedures for rock discontinuity characterization and exploited for the 3D documentation of any part of a rock face. Such dense 3D data, especially LiDAR point clouds, are being used ever more widely, notably for determining discontinuity orientations (Lato et al., 2010; Duan et al., 2011; García-Sellés et al., 2011; Assali et al., 2014; Riquelme et al., 2014) and discontinuity spacing (Riquelme et al., 2015), even for large scale applications (Hilley et al., 2010).

However, although the acquisition phase is highly automated, managing, handling and exploiting such great amount of collected data is an arduous task and especially for non specialist users. The conversion of point clouds data into useful information for the need of rock engineering practices is therefore a crucial issue.

This paper presents our approach to overcome this issue and discusses the solid image principle as a support for geostructral mapping and key block modeling. The concept of solid image is described and its implementation into a standalone software is discussed. Various tools are tested and illustrated thanks to a case study in a limestone quarry.

2. The concept of solid image

2.1. Definition

Bornaz and Dequal (2004) introduced the notion of "solid image" as the enrichment of a classical 2D digital image with the corresponding 3D geometrical information, e.g. a laser-scanning or photogrammetric point cloud. For all practical purposes, it is widely accepted that the geometrical data is not basically stored into different layers-for the coordinates components -, but are preferentially supplied thanks to a single range matrix-or depth map layer-for maximizing computing capacity (see Fig. 1).

In addition to range data, other sets of information can also be added to the previously described Solid Image. For instance, in case of a scanner-laser point cloud, reflectivity values may be available and could therefore be also associated to the corresponding pixel on the 2D image. This value is related to the material's reflection factor and can be of fundamental importance for further analysis-type of material, water seepage, etc. Sometimes, we also have structural information available thanks to automated processes for classifying the point cloud according to the discontinuity sets orientations. Through a specific color palette, main extracted discontinuity sets can then be projected onto the image, helping with the structural interpretation and thus improving the outcrop understanding. In case of a thermographic survey, using for instance an Infra-Red sensor, the temperature information could also be added on a specific additional layer as a further enrichment of the solid image.

Gathering 3D information and 2D images requires an accurate knowledge of internal and external parameters of the considered camera. The location, orientation and lens distortions are computed through a first calibration step.

2.2. Image calibration

The calibration process consists of the computation of the internal orientation parameters for a considered camera. These intrinsic parameters encompass focal length, image format, principal point offset and lens distortions (Hartley and Zisserman, 2004). Traditionally, the camera calibration is performed by measuring, on a image sequence, a set of sufficient 3D control points, which are previously and accurately surveyed by geodetic means. To help with this process, a "calibration corner" composed of sixty six coded targets, disposed in a 3D space, has been created (see Fig. 2).

Once the control points' coordinates are defined, the camera calibration parameters can then be accurately estimated by using a classic bundle adjustment (Hartley and Zisserman, 2004).

2.3. Point cloud projection

Creating a solid image requires a co-registration of the camera and the 3D model. This can be ensured by surveying a few control points, marked on both image and 3D model. Assuming this prerequisite is done, the first step for solid image production consists in projecting each 3D point onto the corresponding image plane. The mathematical model used to compute image coordinates for each 3D point is based on the well-known collinearity equations including radial distortions components (Hartley and Zisserman, 2004).

Thanks to these standard equations, the range image is built and image pixels are now associated to the corresponding 3D points. Considering the geometrical relation between the "object" space and the "image" space, as illustrated in Fig. 3, the 3D spatial position of each pixel can be easily retrieved.

In the camera system, each pixel corresponds to a spatial direction given by two angles, α and θ, determined as:

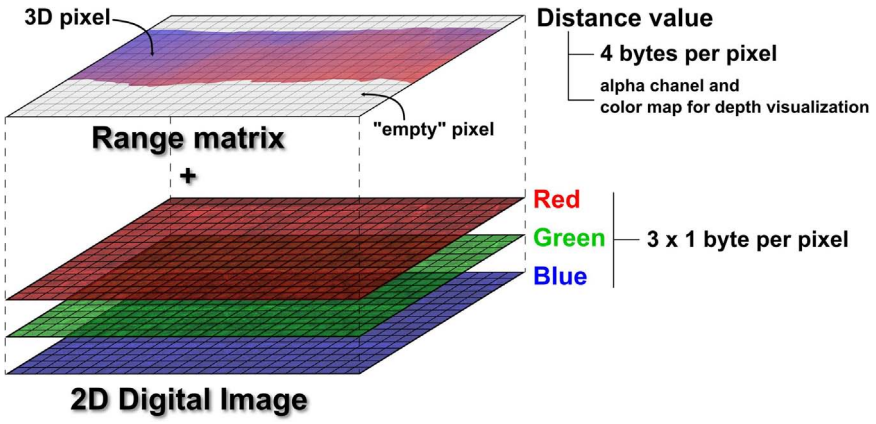

Fig. 1. The solid image concept: basic structure and multiple layers-Three layers for the true RGB color and one range matrix corresponding to the 3D geometrical information. Here, the range value is also color coded for visualization purposes.

Fig. 2. Calibration corner, coded targets and internal parameters – (a) The calibration corner is composed by 66 coded targets. (b) Main camera parameters computed during the calibration process.

$$\begin{cases} \alpha = \arctan\left(\dfrac{x_{ip}}{f}\right) \\ \theta = \arctan\left(\dfrac{y_{ip}}{\sqrt{f^2 + x_{ip}^2}}\right) \end{cases} \quad (1)$$

Where: - α is the horizontal angle.

θ is the vertical angle.
f is the focal length.
x_{ip} and y_{ip} are the image coordinates of the studied point.

Range data are then used to compute the spatial position of the corresponding points in the camera system. Finally, we apply an affine transformation with six parameters to retrieve the points coordinates in the general reference system.

$$\begin{pmatrix} X_P \\ Y_P \\ Z_P \end{pmatrix} = \begin{pmatrix} X_0 \\ X_0 \\ X_0 \end{pmatrix} + R_{\omega\varphi\varphi} \cdot \begin{pmatrix} D.\ \cos(\theta).\ \sin(\alpha) \\ D.\ \sin(\theta) \\ -D.\ \cos(\theta).\ \cos(\alpha) \end{pmatrix} \quad (2)$$

Where: - X_0,Y_0,Z_0 are the coordinates of the perspective centre.

$R_{\omega\varphi\chi}$ is the rotation matrix describing the camera orientation.
D is the range value, i.e. the distance between the camera position and the considered point.
α and θ are the angles previously described in Eq. (1).
X_P,Y_P,Z_P are the object coordinates of the considered point.

2.4. Limitations, interpolations and filtering

The spatial density of a digital image is most of the time much higher than the density of the 3D point cloud. In the final solid image, three main disorders result from this sampling gap.

First of all, it may occur that multiple 3D points are projected onto the same 2D pixel. In that case, we keep only the closest point by approximating that the others points are hidden by this one.

Unlike this first phenomenon, a second occurrence is more frequently observed. Due to the sampling gap, the range matrix is not completely filled and some areas of the image remain without any geometrical information. In order to make the solid image homogenous and to fill the distance matrix, it is thus necessary to integrate the missing values with an interpolation process. Classical convolution matrix can be used for this purpose, employing the "Inverse Distance Weighting" (IDW) method. The assigned values to unknown pixels are calculated with a weighted average of the values available in the neighborhood using the formula:

$$D_{(x,y)} = \frac{\sum_{i=1}^{n}\left[\frac{D_i}{d_i^p}\right]}{\sum_{i=1}^{n}\left[\frac{1}{d_i^p}\right]} \quad (3)$$

Where: - x and y are the image coordinates of the current "empty" pixel.

n is the number of considered points in the neighborhood.
p is the power parameter of the interpolation.
d_i is the image distance between the "empty" pixel (x,y) and the considered pixel i.
D_i is the range value corresponding to the considered pixel i.

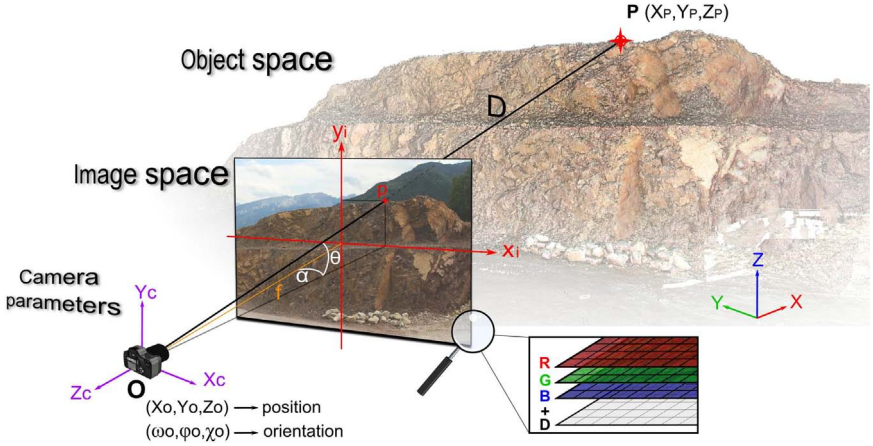

Fig. 3. The solid image concept: geometrical relation between *"Object"* space and *"Image"* space for computing the corresponding 3D position of any pixel of the digital image. Both image and 3D point cloud have to be expressed in the same reference system. Inspired by Bornaz and Dequal (2004).

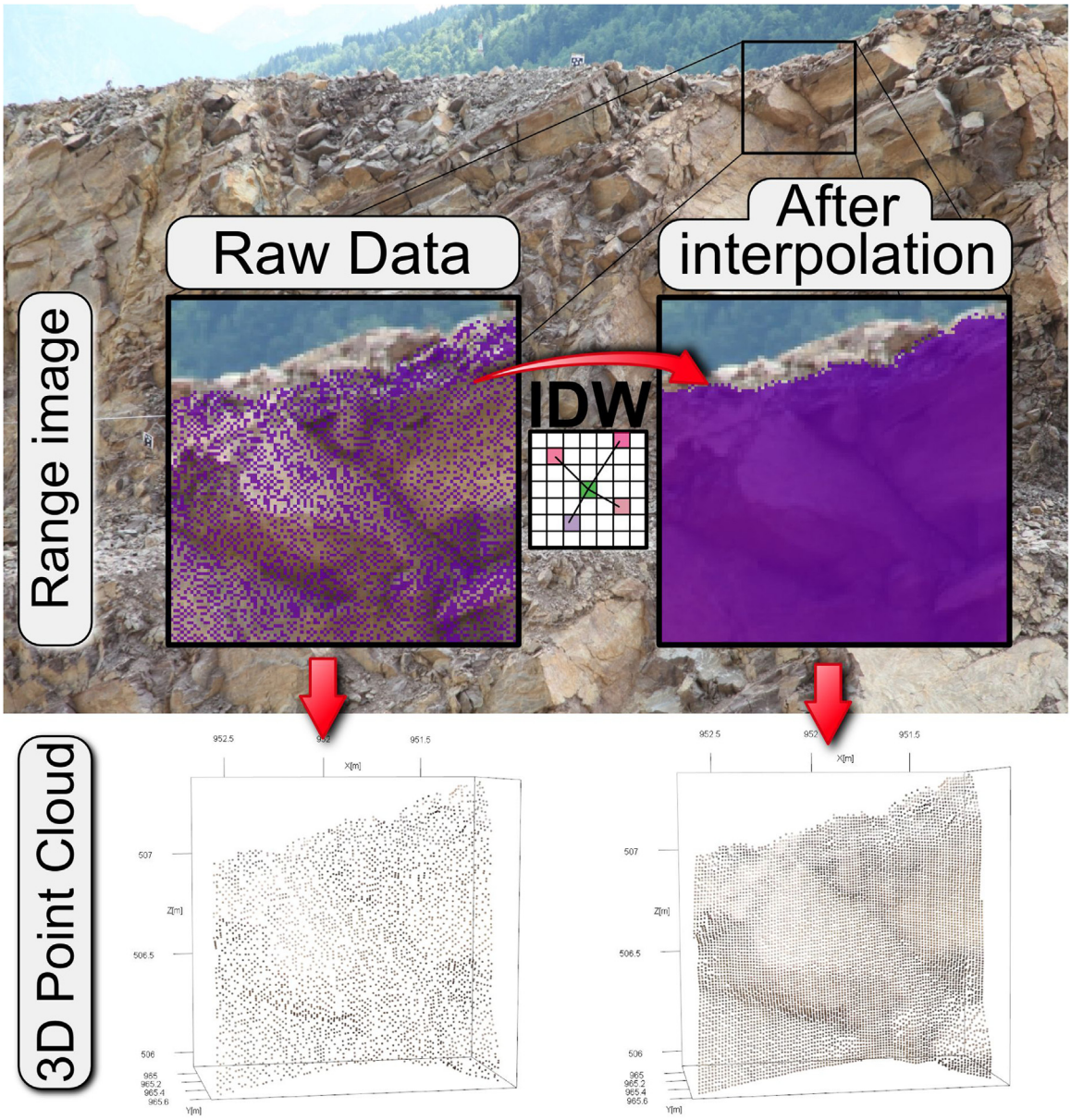

Fig. 4. Spatial interpolation using the *"Inverse Distance Weighting"* method. The impact of the interpolation process is illustrated on both range image and corresponding 3D point cloud.

An illustration of the impact of a spatial interpolation using this methodology is given in Fig. 4.

Another imperfection of the produced solid image occurs when hidden points are still projected onto the image plane. This shortcoming can be repaired by applying a distance based conditional filter. The entire image is scanned with a classical search matrix (3×3, 5×5 or larger) loading the distance information. The minimum distance (D_{min}) observed within the search matrix and the local resolution (r, side of the pixel) are computed. Then the pixel for which $D_{(x,y)} > D_{min} + sf.\ r$ are considered hidden points and canceled out. sf is a sensitivity factor allowing an adaptive adjustment of the tolerance threshold on the range local variation. Munaretto and Roggero (2013) give 2 or 3 as defaults values providing acceptable results for solid image enhancement.

The concept of solid image, as previously described, has been implemented for the need of our research. The following sections describe the developed approach and the actual achievements, considering the solid image as a support for carrying out a geostructural mapping and key block modeling.

3. Implemented software for creating and managing a solid image sequence

A specific software package has been developed in a combination of C++ and R[1] code to create, manage and exploit solid image sequences for fracture mapping and key block modeling purposes. Implemented tools have been included in the *Gaia-GeoRoc* software. *Gaia-GeoRoc* was developed by the authors since 2012 and is intended for processing 3D point clouds and calibrated

[1] R is a language and environment for statistical computing and graphics – http://www.r-project.org/.

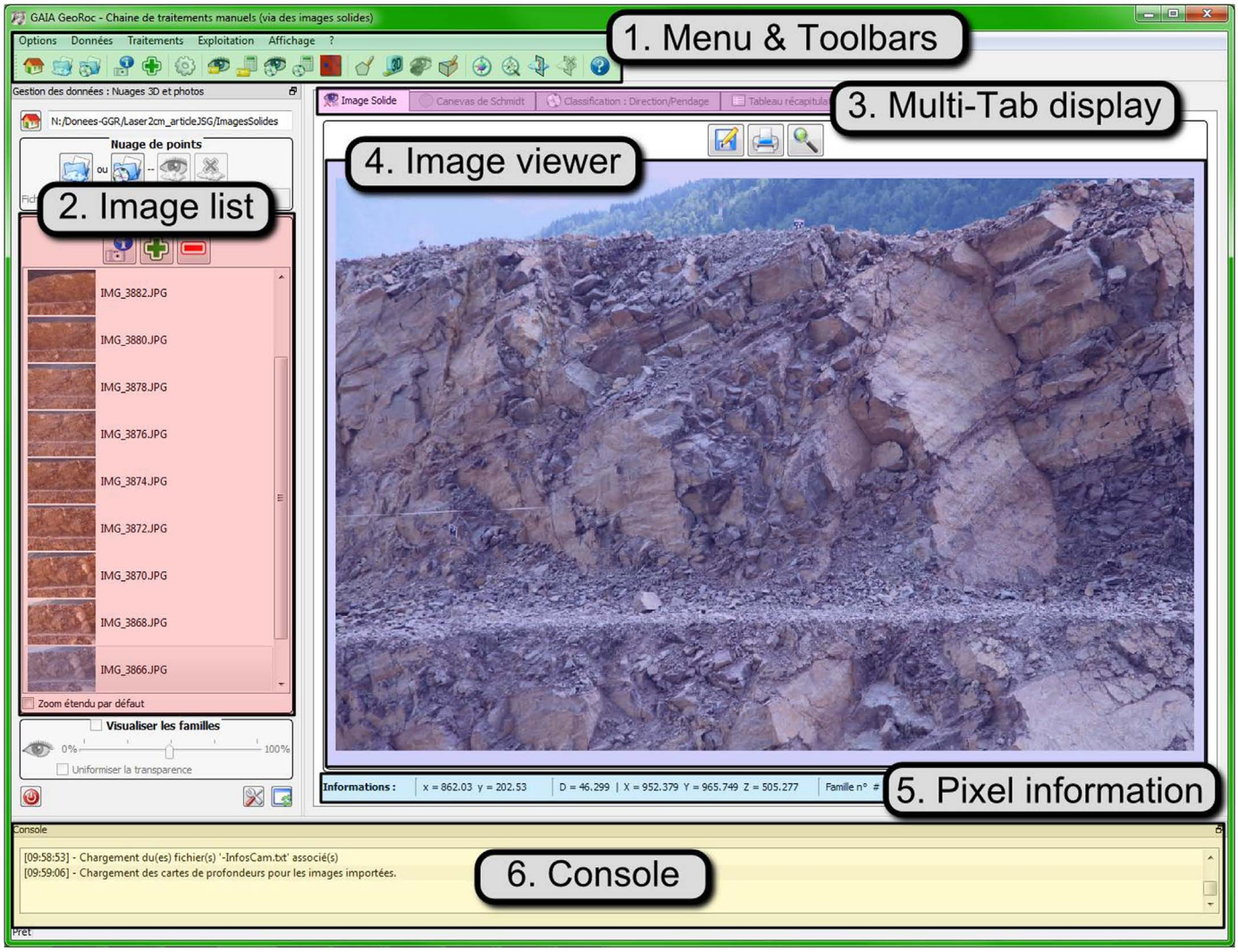

Fig. 5. Presentation of the graphical user interface implemented for creating, managing and exploiting sequences of solid images (annotated screen shot).

images for rock mass characterization. It allows the processing of laser-scanning or photogrammetric point clouds, and includes a semi-automated procedure for discontinuity sets recognition through a orientation based classification algorithm (Assali et al., 2014). *Gaia-GeoRoc* is freely available on e-mail request from the SNCF engineering management and has been deposited with the APP[2]. The built-in graphical user interface is illustrated in Fig. 5.

Gaia-GeoRoc produces and manages multiple-layer solid images (9 bytes per pixel).

The developed tools allow to build the expert assessment step by step as discussed in greater detail in the following section.

4. Structural mapping

The complete procedure, from the camera calibration to the solid image exploitation has been performed on different sites and especially on a limestone quarry located near the town of Saint–Jeoire, in Haute–Savoie, France (Assali et al., 2014). The results obtained with the solid image approach could therefore be compared with the already established structural statement.

The laser scanning survey has been performed with a *Leica HDS7000* device and a spatial density of 1600 pts/m^2, i.e. with approximately 2 cm separating two contiguous points in the 3D model. We have worked on an 11 image sequence acquired using a calibrated *Canon EOS 5D Mark II* camera with a 105 mm lens. The images have been downsampled to be in accordance with the spatial resolution of the point cloud to finally make a pixel at the rock surface about 1.3 cm. Using coded targets as control points *(not necessary on the rock surface)* enabled us to co-reference 2D images and 3D laser point cloud.

Due to the rock slope geometry of this case study, the hidden points filtering process was not needed. On the other hand, eliminating the sampling disparity between images and point cloud, a single IDW interpolation step (see Eq. (3)) has been carried out with 4 considered points in the neighborhood (n) and a power parameter of 2 (p). These values have been chosen in order to make the data homogenous and to correctly fill the distance matrix. The solid images were then ready to be exploited.

4.1. 3D real-time information

Classical image processing software allow the user to easily access image coordinates and color components by just moving the cursor onto the image. *Gaia-GeoRoc* and solid images provide some further information in the same way. Directly readable from

[2] European body for protecting authors' and publishers' digital works – http://www.app.asso.fr/en/welcome.html.

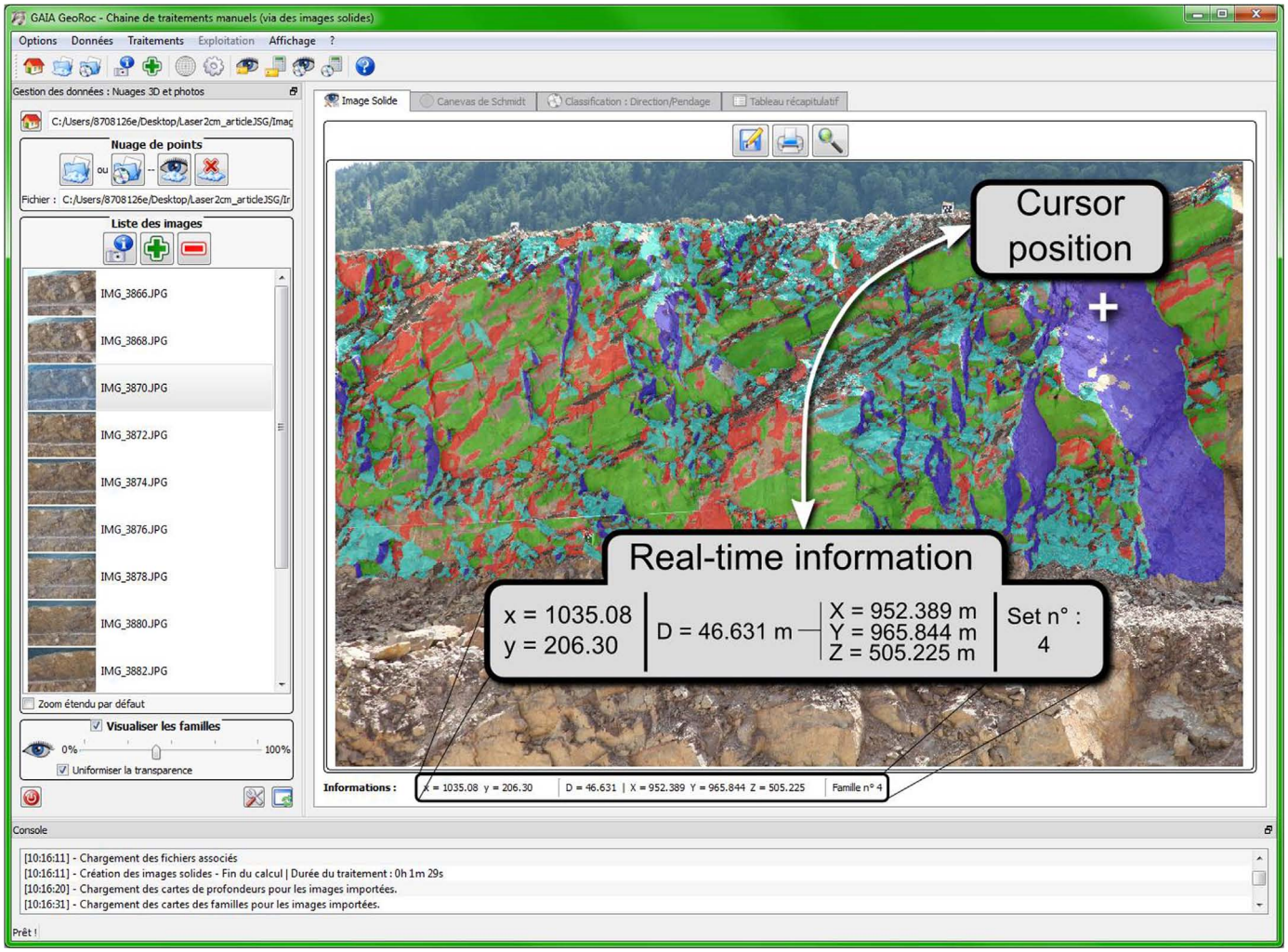

Fig. 6. Example of a solid image in the graphic interface developed as part of this research (annotated screen shot). Colors corresponding to discontinuity sets are projected onto the digital image and real-time information is updated according to the cursor position. The variable transparency factor for the color projection is user-defined at the bottom of the left tool frame.

the image structure, the range value and the discontinuity set index, if available for the considered pixel, are also displayed in the *'pixel information'* frame right below the studied image. In addition, using this distance value and the camera parameters, the 3D coordinates of the corresponding point are computed and displayed in the same time-see Fig. 6.

4.2. Digital survey for discontinuity sampling

Solid image makes it possible to carry out correct three-dimensional measurements of any part of the digitized rock face by just selecting points on the image. 3D distance measurements between two selected points are therefore easily performed. A dedicated inspection wizard has been also developed, automatically converting 2D pixels selections into useful information for the need of rock engineering practices. Each inspection object is labeled and stored in a dedicated list placed next to the surveyed image. An illustration is given in Fig. 7.

Once an inspection area has been selected, in polyline or polygon mode, a planar best-fit on the corresponding point cloud is used to compute the spatial orientation, in terms of strike and dip, or dip direction and dip. Spatial orientations are automatically added to the stereoplot available in the second tab of the central pane. The 3D set of clicked points is then projected onto this resultant plane in order to calculate the surface (or the length) of the selected area. A three-dimensional view of each inspected zone is also available helping with the rock face understanding. Finally, for each measurements area, the software provides the operator with the following properties:

- Number of pixels;
- Number of corresponding 3D points;
- Surface of the polygonal area, or length of the fracture's trace;
- Strike and dip (or dip direction and dip);
- Standard deviation from the mean plane. This gives some information about the planarity of the selected zone.

As already mentioned, several methods were used on the limestone quarry site to perform the structural survey. Traditional compass–clinometer survey highlighted 4 discontinuity sets, whereas 5 clusters were clearly characterized from the 3D laser data thanks to a semi-automated classification process (Assali et al., 2014). As laser scanning always provides larger data samples than traditional compass surveys and allows data to be obtained for much larger areas of a rock face, this structural diagnosis was validated and we considered it a reference.

As part of our case study, we also tested the use of solid images in a structural survey by inspecting 10 measurement areas on an image sequence for each of the 5 previously spotted and validated discontinuity sets. Selection of the measurement areas, done by a

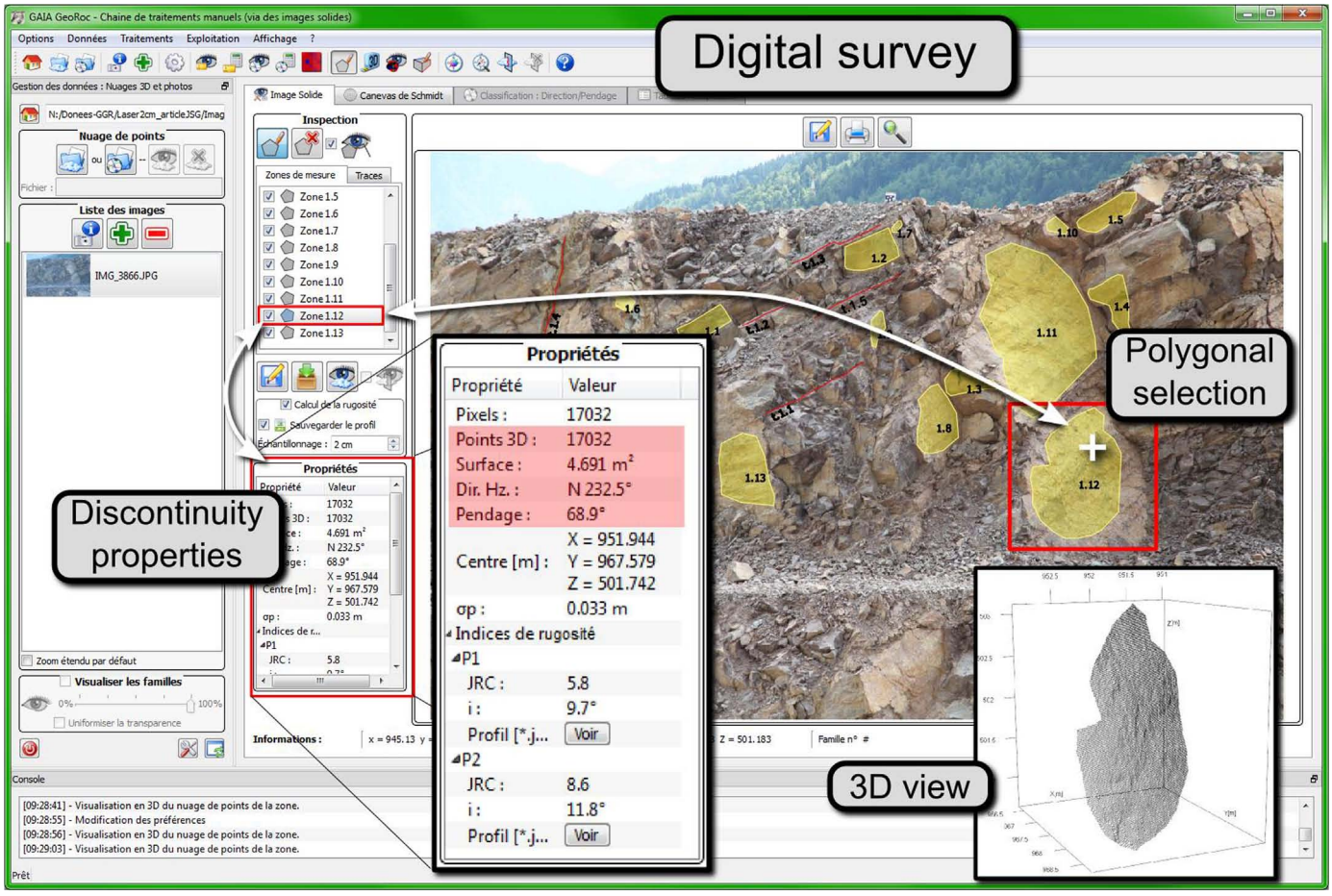

Fig. 7. Manual discontinuity sampling: digital survey and properties extraction. Pixels selection can be performed using polylines or polygons for both fracture traces and facets.

geologist operator, was facilitated by projecting the color for each discontinuity set onto the image.

Resulting stereonets, for the 3 methodologies, are shown in Fig. 8. The solid image stereonet (Fig. 8(c)) completely matches the validated results (Fig. 8(b)). The reliability of solid image for orientation measurement of visible discontinuities is then established.

In addition to orientation parameters, the proposed software also integrates an estimation of the roughness of rock surfaces for the inspected zones.

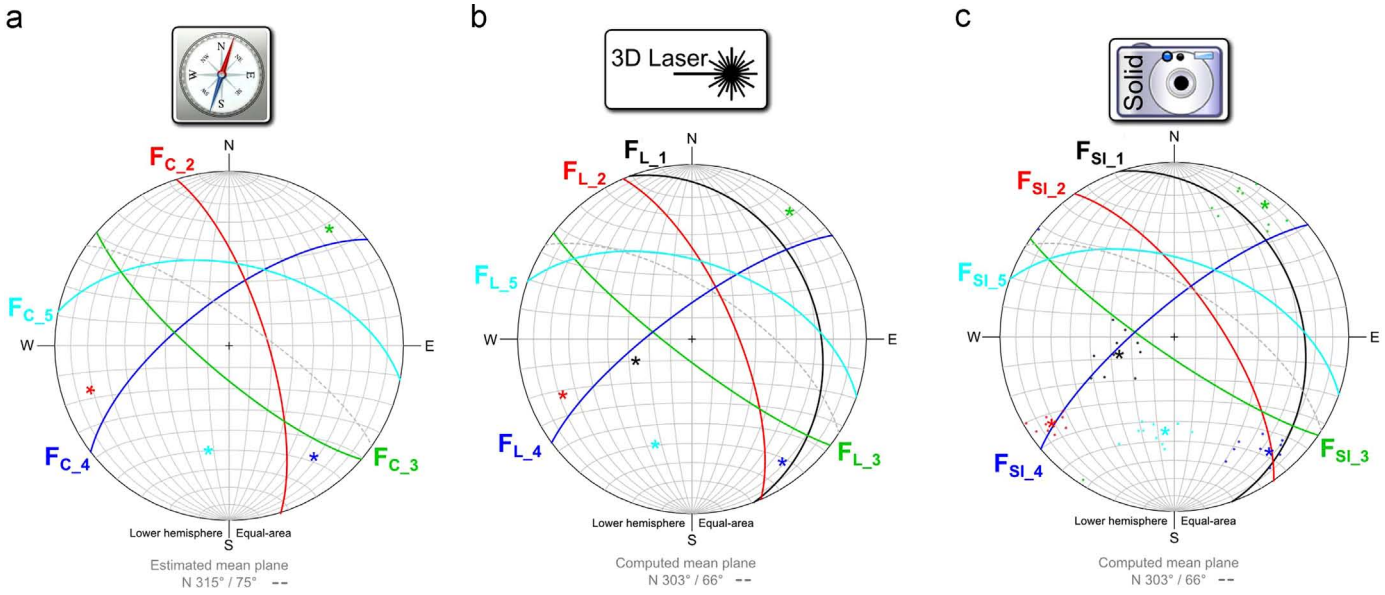

Fig. 8. Comparison of orientation measurement with different techniques: From left to right, the stereonets are the result of: a classical compass survey, an automated 3D point cloud classification, the solid image based survey.

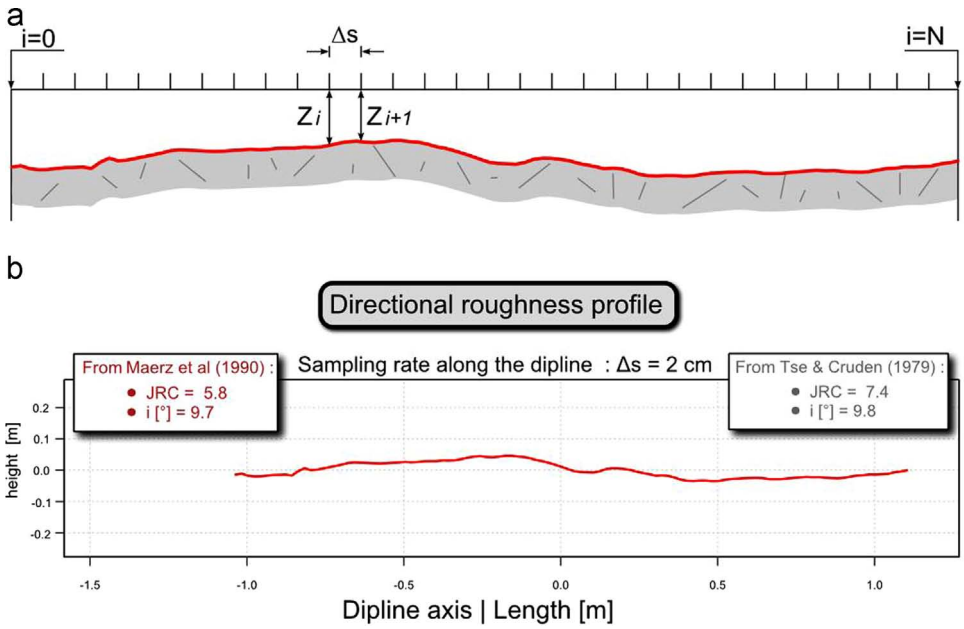

Fig. 9. Evaluation of joint roughness parameters-(a) Procedure for measuring roughness with 2D directional profile-Inspired by Wyllie et Mah (2004). (b) Example.

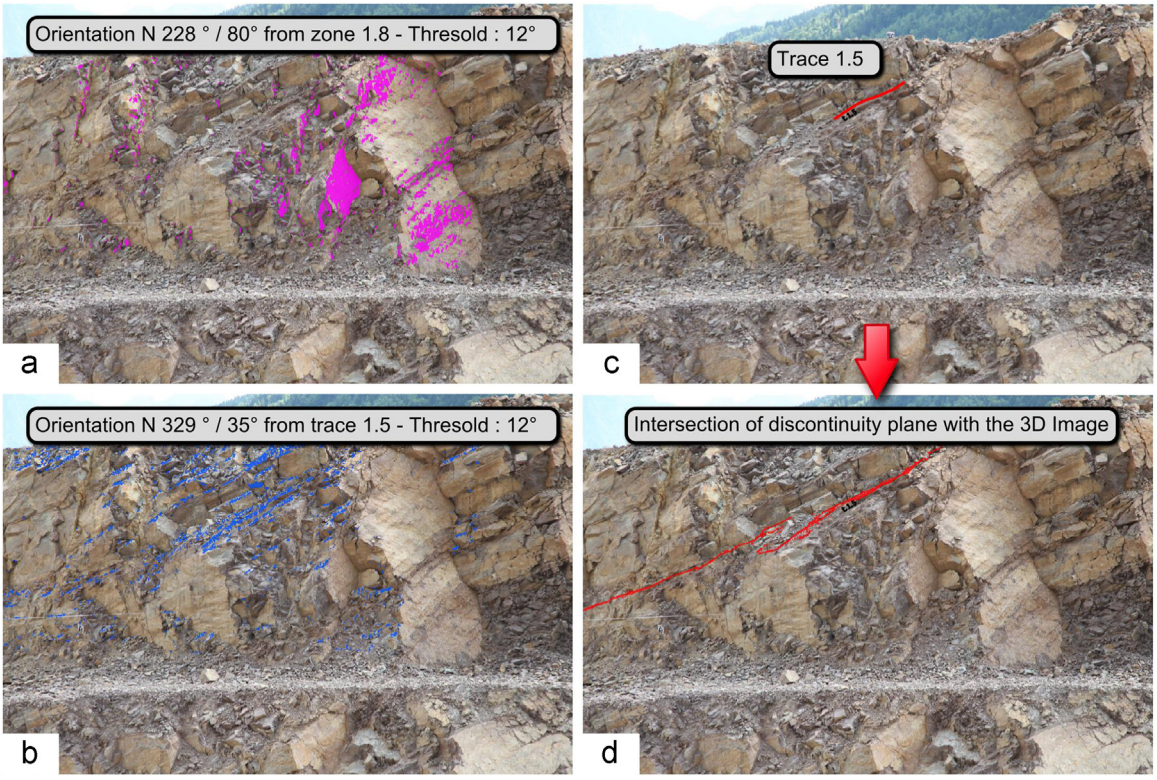

Fig. 10. Enhancement of structural interpretation – (a) Highlighting a specific orientation on the image. (b) Visualization of the intersection/propagation of any discontinuity plane with the rock mass.

4.3. *Directional roughness estimation*

Traditional methods for practical measurement of rock surface roughness generally require direct contact with the rock face. Both laboratory and field methods can produce accurate and useful results but the need of a direct access to the outcrop is a quite significant limitation. Using a mechanical profilometer (Tse and Cruden, 1979) or a shadow profilometer with a video camera (Maerz et al., 1990), quantitative methods of profile measurement were established. Based on these principles, Haneberg (2007) proposed an adapted digital method for the computation of directional roughness profiles from three-dimensional point clouds.

We built on this research to integrate such an estimate within the proposed digital survey approach. The point cloud is interpolated onto a regular grid on the mean plane using bicubic splines, with a user-defined sampling rate. Two profiles are extracted, one along the dip-line axis and another along the strike direction.

For each digital profile consisting of N discrete points separated by distance Δs and having heights Z_i measured from a single

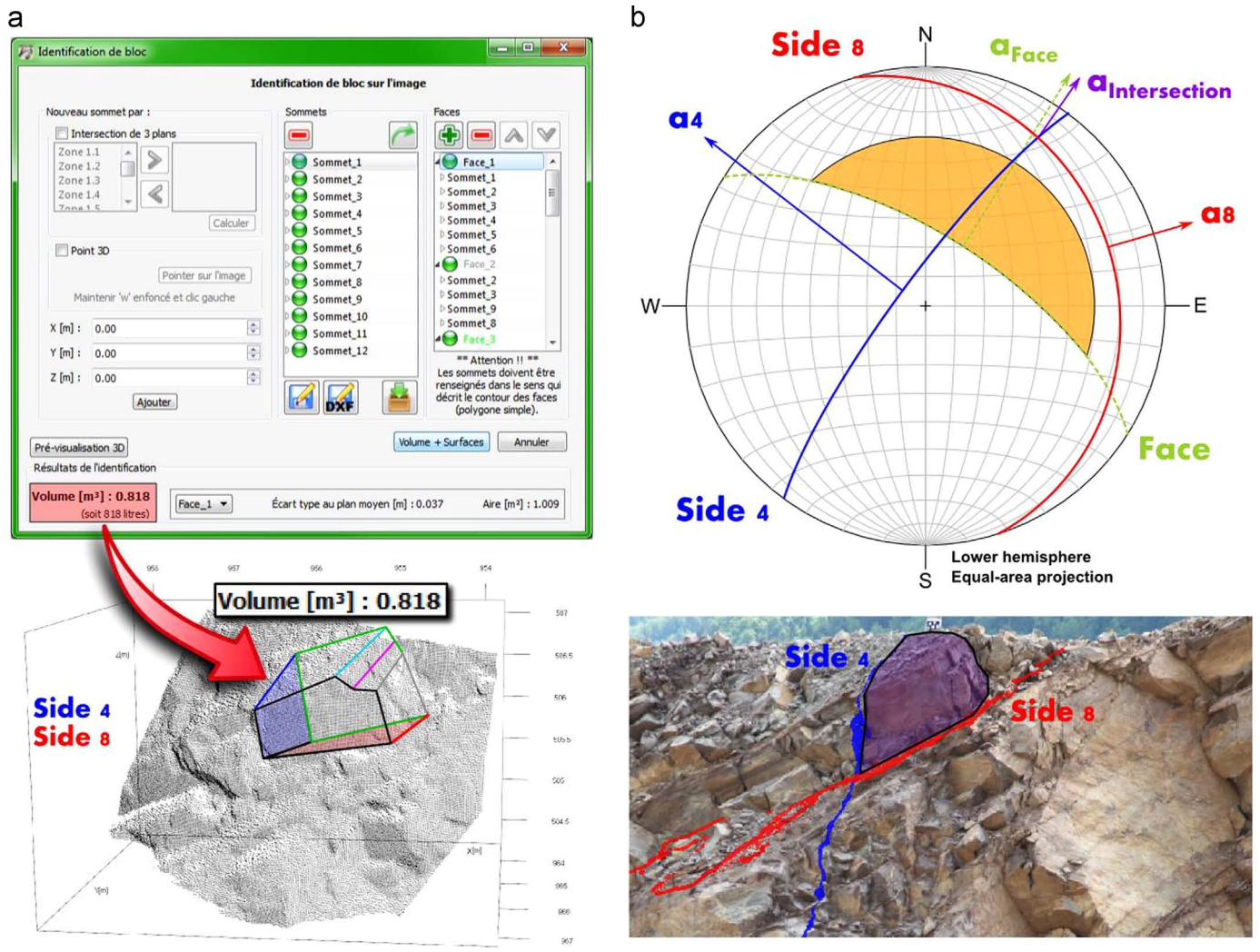

Fig. 11. Key bloc modeling-Example (1) – (a) Modeling wizard for the studied block and corresponding 3D preview in the point cloud. (b) Kinematic analysis and spatial configuration of the block at the rock surface.

reference height (see Fig. 9), Joint Roughness Coefficient (JRC) and asperity angle (i) are calculated thanks to the following empirical correlations given by Maerz et al. (1990):

$$JRC = c.\,(R_p - 1) \quad and \quad i = \arccos\left(\frac{1}{R_p}\right) \tag{4}$$

$$R_p = \frac{\sum_{i=0}^{N-1}\sqrt{\Delta s^2 + \left(Z_i - Z_{i+1}\right)^2}}{\Delta s.\,(N-1)} \tag{5}$$

where c is an empirical constant with a given default value of 401.

Other similar empirical correlations developed by Tse and Cruden (1979) are applied in the same way in order to strengthen the roughness estimation process. The visual comparison of *JRC* standard profiles with the digitally extracted ones shows that the numerical roughness estimates, i.e. *JRC* and *i*, are quite consistent with type curves of that roughness. Even if field control remains essential in practical applications, the ability of this digital method to estimate directional surface roughness on a scale comparable to the size of potentially unstable blocks rather than small samples is a significant advantage.

After each surveyed area has been fully characterized, with all the previously mentioned properties (orientation, roughness, etc.), the analysis is then focused on the geometrical structure of these discontinuities, in order to identify and describe potentially unstable key blocks. For this purpose, the tool we propose is designed to optimize our understanding of discontinuity planes connections.

4.4. Global connections of discontinuity planes

Since the spatial distribution of the data collected at the surface of the outcrop must be extrapolated to the inner part of the massif, having knowledge of how a specific surveyed discontinuity will interact with the global 3D model is of decisive interest. Two complementary implements are proposed, both helping with structural investigations: a first tool for highlighting specific orientation areas, and a second one which computes the intersection of a given planar feature and displays it directly on the image sequence.

The first application program is intended for computing the local orientation for each 3D pixel and coloring it whether it belongs to a specific searched orientation. When a fracture has been identified and surveyed, this approach can be use to mark all the points with approximately the same orientation at the rock surface. For structural interpretation purposes, a user-defined threshold about the orientation deviation is proposed. On Fig. 10 (b), bedding planes are clearly highlighted by the blue coloration for pixels belonging to the bedding orientation.

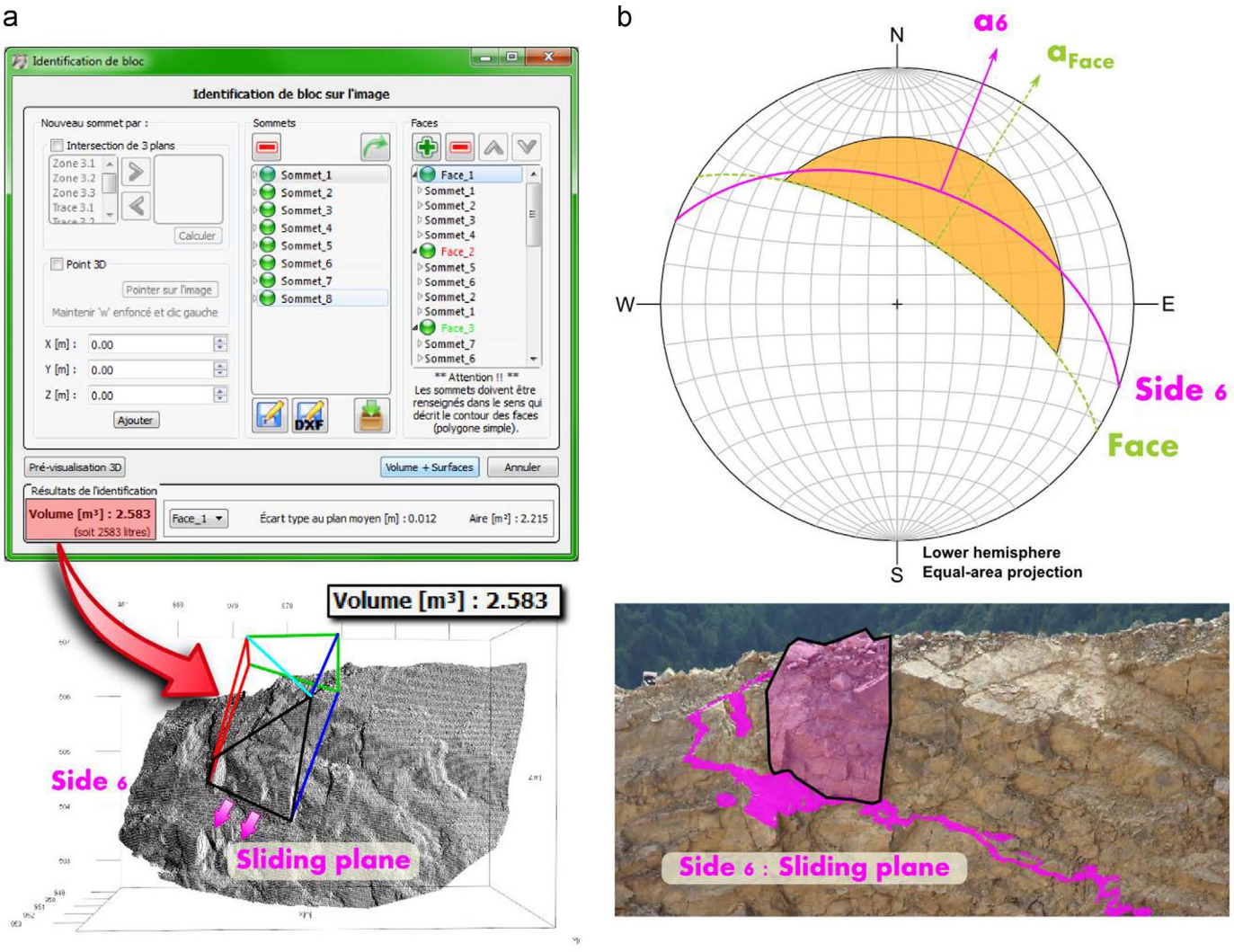

Fig. 12. Key bloc modeling-Example (2).

A further proposed tool deals with the intersection of solid image and planar feature. By highlighting this intersection area, the propagation of a specific fracture, surveyed on the solid image or estimated by geophysical means, can therefore be easily visualized (see Fig. 10(c) and (d)).

The direct display of these propagated fracture planes on the image is a valuable contribution for understanding the individualization of potentially unstable key blocks.

4.5. *Key block modeling*

From a practical perspective, the main issue for structural mapping is to identify unstable rock blocks and quantify the associated risks, by analyzing their location, geometry and the structure of the fractures which individualize them. Considering the rock block theory proposed by Goodman and Shi (1985), many different combinations of discontinuities can be passed over and critical rock blocks are therefore directly inspected. A kinematic analysis is then carried out in order to analyze sliding or toppling possibilities of the studied key blocks.

We built on this principle to propose a built-in key bloc modeling. The approach is based on the well accepted simplification that all blocks are limited by mathematical planes and could be therefore modeled by simple geometric polyhedrons. A specific wizard including a 3D pre-view is then proposed, helping with the modeling process. The volume of the inspected block is thus ready to be computed and the kinematic analysis can be performed.

In the field case study discussed in introduction of Section 4, two different rock blocks have been identified and modeled using the developed procedure. The modeling interface and the corresponding 3D view, for the two blocks, are shown in Figs. 11(a) and 12(a).

Analyzing the first block configuration, as shown on Fig. 11(b), the mode of slope instability has been identified as a wedge failure. The interpretation of sliding possibilities is performed thanks to the stereoplot. In this case, assuming that the only force acting on the block is gravity, the inclination of the line of intersection is not sufficient to destabilize the block. But, considering that stability is guaranteed as long as the sum of the resisting forces is higher than the driving forces, this stable situation may be ephemeral. A material degradation producing a reduction of the shear strength, or variable hydraulic constraints within the massif, could make this potentially critical bloc a real key bloc.

The second example illustrates another type of rock failure involving only one simple slide plane. This configuration is illustrated in Fig. 12(b). Assuming that the two lateral boundaries of the block are defined by release surfaces with negligible resistance, and that the upper end of the sliding surface (*side 6*) terminates in a tension crack, sliding possibilities can be inspected. It appears that sliding is kinematically feasible and may occur for

this bloc. This information is of crucial importance and can then be used to choose the most appropriate and most cost-effective risk-treatment measures.

If these kinematic analyses definitely require further developments and automation, this kind of application does illustrate the tool's potential for key bloc modeling and structural diagnosis. On this point, the proposed achievements are the basis of an ongoing research.

5. Conclusion

This paper describes a computational approach for 3D mapping and geostructural survey and analysis thanks to the combination of 3D point clouds and 2D digital images. Based on the concept of solid image, a new software-*GAIA-GeoRoc*-has been developed and validated on a typical field case study. In comparison to classical survey data which are affected by many deficiencies (lack of data and sampling difficulties due to inaccessible areas, safety risk in steep sectors, etc.), the reliability of the proposed digital survey approach has been proved. Considering the solid image as a support for geostructural mapping and key block modeling, one of the major asset is the improvement of the safety conditions during the survey-especially in road or railway environment. No direct access to the studied rock face is needed and the analysis is performed directly on a single computer station using all benefits of 3D data combined with the geologist knowledge. For the naturalist-geologist, the direct visualization on the image of three-dimensional structures and phenomena is a serious contribution for structural interpretation and thus for the trustworthiness of his analysis.

The interests are at once:
technical: improving the quality of the products and performing further analysis;
safe: avoiding or reducing the needs of direct access to the rock face during the surveys;
economic: reducing the time required for field surveys, and data processing at the office, without any return on the study site. Geometrical information extracted from the solid images helps for determining the most appropriate and the most cost-effective risk-treatment measures, especially during the design process.

In addition to the tools presented in this paper, *GAIA-GeoRoc* also includes the following feature: advanced visualization of 3D point clouds, semi-automatic extraction of discontinuity sets through direct segmentation and determination of persistence and spacing parameters. The software has been developed primarily for geologists in charge of rock fall risk management along the French railway network.

Acknowledgments

This project was carried out as part of a doctoral research project supported by SNCF (French National Railway Company),for improving the risk management methodologies related to linear outcrops along the railway network. The authors would like to thank SNCF's Engineering and Research & Innovation Departments, as well as the engineering company IMSRN (Ground Movement and Natural Hazards Engineering) in Montbonnot-Saint Martin (Isère, France), INSA de Strasbourg, and the University of Savoie for their active assistance with fieldwork. The authors also would like to thank the two reviewers and editor for their contribution to this paper.

References

Assali, P., Grussenmeyer, P., Villemin, T., Pollet, N., Viguier, F., 2014. Surveying and modeling of rock discontinuities by terrestrial laser scanning and photogrammetry: semi-automatic approaches for linear outcrop inspection. J. Struct. Geol. 66, 102–114.

Bornaz, L., Dequal, S., 2004. The solid image: An Easy and Complete Way to Describe 3D Objects. In: XXth ISPRS congress, Istanbul. 12–23 July 2004, Vol. XXXV, part B5, pp. 432–437.

Buckley, S., Howell, J., Enge, H., Kurz, T., 2008. Terrestrial laser scanning in geology: data acquisition, processing and accuracy considerations. J. Geol. Soc. 165, 625–638.

Duan, Y., Xiaoling, L., Maerz, N., Otoo, J., 2011. Automatic 3D Facet Orientations Estimation from LIDAR Imaging. Engineering Research and Innovation Conference, Atlanta, Georgia.

García-Sellés, D., Falivene, O., Arbués, P., Gratacos, O., Tavani, S., Muñoz, J.A., 2011. Supervised identification and reconstruction of near-planar geological surfaces from terrestrial laser scanning. Comput. Geosci. 37, 1584–1594.

Goodman, R.E., Shi, G.-h., 1985. Block theory and its application to rock engineering. In: civil engineering and engineering mechanics. Englewood Cliffs. Prentice-Hall. ISBN 0-13-078189-4.

Haneberg, W. C., 2007. Directional roughness profiles from three-dimensional photogrammetric or laser scanner point clouds. In: Proceedings of the 1st Canada, U.S. Rock Mechanics Symposium, Vancouver, May 27–31.

Hartley, R., Zisserman, A., 2004. Multiple View Geometry in Computer Vision. Cambridge University Press, Cambridge, ISBN: 0521540518.

Hilley, G.E., Mynatt, I., Pollard, D.D., 2010. Structural geometry of Raplee Ridge monocline and thrust fault imaged using inverse Boundary Element Modeling and ALSM data. J. Struct. Geol. 32, 45–58.

Kemeny, J., Post, R., 2003. Estimating three-dimensional rock discontinuity orientation from digital images of fracture traces. Comput. Geosci. 29, 65–77.

Lato, M., Diederichs, M.S., Hutchinson, D., 2010. Bias correction for view-limited lidar scanning of rock outcrops for structural characterization. Rock. Mech. Rock. Eng. 43, 615–628.

Maerz, N.H., Franklin, J.A., Bennett, C.P., 1990. Joint roughness measurement using shadow profilometry. Int. J. Rock. Mech. Min. Sci. Geomech. Abstr. 27, 329–343.

Munaretto, D. Roggero, M., 2013. Solid Image Extraction From Lidar Poind Clouds. In: International Archives of the Photogammetry, Remote Sensing and Spatial Information Sciences. Volume XL-5/W1, 189–195.

Priest, S., Hudson, J., 1981. Estimation of discontinuity spacing and trace length using scanline surveys. Int. J. Rock. Mech. Min. Sci. Geomech. Abstr. 18, 183–197.

Riquelme, A.J., Abellan, A., Tomas, R., Jaboyedoff, M., 2014. A new approach for semi-automatic rock mass joints recognition from 3D point clouds. Comput. Geosci. 68, 38–52.

Riquelme, A.J., Abellan, A., Tomas, R., 2015. Discontinuity spacing analysis in rock masses using 3D point clouds. Eng. Geol. 195, 185–195.

Slob, S., Hack, R., vonKnapen, B., Turner, K., Kemeny, J., 2005. Method for automated discontinuity analysis of rock slopes with three-dimensional laser scanning. Trans. Res. Rec. : J. T.R.B. 1913, 187–194.

Sturzenegger, M., et Stead, D., 2009. Close-range terrestrial digital photogrammetry and terrestrial laser scanning for discontinuity characterization on rock cuts. Eng. Geol. 106 (3–4), 163–182.

Tse, R., CrudenD.M., R., 1979. Estimating joint roughness coefficients. Int. J. Rock. Mech. Min. Sci. Geomech. Abstr. 16, 303–307.

Wyllie, D., Mah, C., 2004. Rock Slope Engineering-Civil and Mining. 4th Edition-based on the third editon by E. Hoek and J. Bray. Spon Press-Taylor & Francis Group. ISBN 10:0-415-28000-1.